DMD #34629

Attenuation of Intestinal Absorption by Major Efflux Transporters:

Quantitative tools and strategies using Caco-2 model

Xuena Lin, Suzanne Skolnik, Xiaohui Chen, and Jianling Wang

Metabolism and Pharmacokinetics, Novartis Institutes for BioMedical Research
Cambridge, MA, USA

1

Running title: Strategy, Quantification, Efflux and Intestinal Absorption

Corresponding author:

Jianling Wang, Ph.D

Novartis Institutes for BioMedical Research,

250 Massachusetts Avenue,

Cambridge, MA 02139

Telephone: 617-871-7140; Fax: 617-871-7061

E-mail: jianling.wang@novartis.com

Number of text pages: 22

Number of tables: 4

Number of figures: 3

Number of references: 40

Number of words in the abstract: 203

Number of words in the Introduction: 660

Number of words in the Discussion: 1330

Abbreviations:

ABC, ATP-binding cassette; AQ, absorption quotient; BCRP, breast cancer resistance protein; cLogP, calculated lipophilicity; DDI, drug-drug interaction; ER, efflux ratio; FA, fraction absorbed; GI, gastrointestinal tract; KO, (gene) knock out; LC/MS/MS, liquid chromatography – tandem mass spectrometry; MDR, multidrug resistance; MRP2, multidrug resistance protein 2; NCEs, new chemical entities; PAMPA, parallel artificial membrane permeability assay; P_{app}, apparent permeability coefficient; P-gp P-glycoprotein; P_{PD}, passive diffusion; $P_{efflux,app}$, apparent efflux transport; PSA, polar surface area; SAR, structure-activity relationships; TEER, transepithelial electrical resistance; TSI, transporter substrate index; WT, wild type.

ABSTRACT

Efflux transporters expressed in the apical membrane of intestinal enterocytes have been implicated in drug oral absorption. The current study presents a strategy and tools to quantitatively predict efflux impact on oral absorption for new chemical entities (NCEs) in early drug discovery. Sixty-three marketed drugs with human absorption data were evaluated in the Caco-2 bidirectional permeability assay and subjected to specific transporter inhibition. A four-zone graphical model was developed from apparent permeability and efflux ratio to quickly identify compounds whose efflux activity may distinctly influence human absorption. NCEs in "zone 4" will likely have efflux as a barrier for oral absorption and further mechanistic studies are required. To interpret mechanistic results, we introduced a new quantitative substrate classification parameter, transporter substrate index (TSI). TSI allowed more flexibility and considered both *in vitro* and *in vivo* outcomes. Its application ranged from addressing the challenge of overlapping substrate specificity to projecting the role of transporter(s) on exposure or potential DDI risk. The potential impact of efflux transporters associated with physicochemical properties on drug absorption was discussed in the context of TSI and also previously reported absorption quotient (AQ). In this way chemistry strategy may be differentially focused on passive permeability or efflux activity or both.

DMD #34629

Introduction

Adequate oral absorption is a prerequisite for the majority of drug candidates. While many factors including dissolution, formulation, and food effects are all relevant, oral absorption in humans is predominantly governed by solubility and permeability through the gastrointestinal tract (GI). In general, solubility and permeability are determined by physicochemical properties such as lipophilicity, molecular size, hydrogen bonding strength, and ionization (van de Waterbeemd et al., 1998). The prediction of human oral absorption, however, is relatively complicated, particularly at an early drug discovery stage. Therefore, several *in vitro* tools have been widely utilized to understand the rate limiting steps and develop correlations with absorption. For permeability assessment, parallel artificial membrane permeability assay (PAMPA) and cell-based assays (e.g. Caco-2) are among the frequently used tools. The Caco-2 assay has the advantage of not only addressing passive permeability but also active transport, and particularly efflux transporters that may limit absorption by extruding compound back to the GI lumen.

P-glycoprotein (P-gp), multidrug resistance protein 2 (MRP2) and breast cancer resistance protein (BCRP) are three best studied efflux transporters in the ATP-binding cassette (ABC) family of membrane transporters. Because of their characteristic location at either the entrance or exit side of membrane barriers, it has been widely recognized that these transporters influence drug absorption and disposition as well as efficacy and safety (Giacomini et al., 2006). For example, P-gp plays a role in restricting the oral absorption of substrates such as digoxin in the GI tract (Igel et al., 2007). The brain accumulation of prazosin and imatinib is attenuated by P-gp and BCRP synergistically at the blood brain barrier (Zhou et al., 2009). In addition, P-gp, MRP2, and BCRP are

implicated in efflux transporter-related multidrug resistance (MDR) in many studied tumor cells (Mimeault et al., 2008). More recently, toxicity concerns due to transporter mediated drug-drug interaction (DDI) have emerged, especially for drugs with a narrow therapeutic index or variable bioavailability (Eberl et al., 2007).

Given the impact of efflux transporters on the absorption, disposition and safety of a wide range of drugs, the identification of substrates and understanding of the rate limiting factors *in vivo* are beneficial to drug candidate selection and optimization. However, it remains challenging to estimate how efflux limits *in vivo* exposure quantitatively from *in vitro* data, especially with a paucity of human *in vivo* data and inter-individual variability. Cell-based bidirectional assays such as the Caco-2 assay described here have been widely employed to identify efflux substrates via the efflux ratio (ER) (Polli et al., 2001). With ER, all active transport via one or multiple transporters is considered alongside passive permeation. Multiple reports indicate that ER alone cannot project the impact of efflux (Troutman and Thakker 2003b, Kalvass and Pollack 2007). Further mechanistic studies are required to understand kinetics and dosing strategy for absorption or raise awareness of potential transporter-mediated DDI.

We have previously described a 96-well Caco-2 bidirectional assay which has successfully measured thousands of NCEs (Skolnik et al., 2010). Overall, 30-40% of Novartis NCEs were identified as potential substrates for transporters using the ER. In the present study, we propose a practical strategy to use limited *in vitro* tools for quickly identifying compounds whose efflux activity may influence human absorption. Specifically, a four-zone graphical model based on Caco-2 data and human absorption of marketed drugs has been developed to focus on efflux substrates with low absorption

concerns. We further investigated the activity of three efflux transporters in the GI system: P-gp, MRP2, and BCRP. A new substrate classification standard was introduced, in which both *in vitro* and *in vivo* behaviors of a substrate were considered. This term, transporter substrate index (TSI), achieved both substrate identification and assessment of transporter activity for each compound. Additionally, we integrated the absorption quotient (AQ) into our data analysis to underscore the influence of physicochemical properties on drug absorption. Overall, we intend to create a strategy for lead candidate selection and optimization by presenting the quantitative assessment of potential efflux attenuation on human oral absorption.

Methods

Materials.

Caco-2 cells were obtained from the American Type Cell Culture (ATCC) repository (Manassas, VA). Heat inactivated fetal bovine serum, Dulbecco's Modified Eagle Medium (DMEM) containing GlutaMAX™-I and high glucose, *N*-2-hydroxyethylpiperazine-*N'*-2-ethanesulfonic acid (HEPES) and Trypsin/2.5% EDTA were purchased from Invitrogen (Carlsbad, CA). Non-essential amino acid solution (NEAA 100x), sodium pyruvate solution (100x) were obtained from Hyclone (Logan, UT). Hank's balanced salt solution (HBSS) was obtained from Mediatech, Inc. (Manassas, VA). Multiwell Insert System 96-well (1.0 µm pore size) plates were purchased from BD Biosciences (Billerica, MA). Six-well Transwell polycarbonate membrane inserts were ordered from Corning (Acton, MA). All solvents were analytical grade and standard test compounds were obtained from Sigma-Aldrich (St. Louis, MO). LY335979, MK571, and Ko143 were obtained in-house, or ordered from Alexis (San Diego, CA) and Pharmabridge Inc. (Doylestown, PA) and utilized without further purification.

Bi-directional transport assay and bioanalysis.

96-well Caco-2 plates with TEER values >200 ohm·cm^2 were used for the assay. Test compounds in transport buffer were added to the donor compartments of either apical (A-B) or basolateral wells (B-A) of the Insert System followed by incubation at 37°C for 120 min. The selection of Caco-2 loading concentration (10 µM) was validated earlier (Skolnik et al., 2010). It was a compromise of allowed solubility, proper identification of efflux substrates in the context of their *in vivo* impact, and exceeding LCMS detection

limit for most discovery NCEs. In inhibition study, cells were first incubated with transport buffer in the presence or absence of inhibitors for 30 minutes at 37°C. The transport buffer was then removed and replaced with new buffer containing test compounds with or without inhibitors. LY335979, MK571 and Ko143 were used to inhibit P-gp, MRP2 and BCRP at 1 µM, 10 µM, and 1 µM respectively (Dantzig et al., 1996; Gekeler et al., 1995; Allen et al., 2002). Samples were collected at 0- and 2-hour time points. Lucifer yellow was added to confirm the membrane integrity following sample collection. Acetonitrile was applied to precipitate proteins and a final analytical plate was created after centrifugation by collecting the supernatant. The analysis of samples was performed on a high performance liquid chromatography – tandem mass spectrometry (LC/MS/MS) system (Skolnik et al., 2010).

Quantitative assessment of efflux influence.

Three quantitative terms were utilized to evaluate the impact of efflux on absorptive transport, including efflux ratio (ER), absorption quotient (AQ) and a new term, transporter substrate index (TSI). To apply each term, apparent drug permeability (P_{app}) across Caco-2 cell monolayers was first determined according to Eq. 1:

$$P_{app} = \frac{dQ}{dt} \bullet \frac{1}{AC_0} \qquad (1)$$

where dQ/dt is the total amount of test compound transported to the acceptor chamber per unit time, A is the surface area of the transport membrane (0.0804 cm^2), and C_0 is the initial compound concentration in the donor chamber.

The ER was determined from the ratio of P_{app} in secretory (B-A) and absorptive (A-B) directions and was used to flag efflux activity when ER $\geq$2 in our laboratory (Skolnik et

DMD #34629

al., 2010). P_{app} in both directions, along with ER, is a function of passive diffusion (P_{PD}) and active transport. For simplicity, the apparent permeability mediated by influx is not considered in the scope of this paper, rendering Eqs. (2- 3):

$$P_{app}(A\text{-}B)= P_{PD}(A\text{-}B) - P_{efflux, app}(A\text{-}B) \qquad (2)$$

$$P_{app}(B\text{-}A)= P_{PD}(B\text{-}A)+ P_{efflux, app}(B\text{-}A) \qquad (3)$$

$P_{PD}(A\text{-}B)$ and $P_{PD}(B\text{-}A)$ are the passive diffusion-mediated apparent permeabilities , which equate to $P_{app}(A\text{-}B)$ and $P_{app}(B\text{-}A)$ when the ER decreased to ≤ 2 in the presence of inhibitor in the current study. $P_{efflux, app}(A\text{-}B)$ and $P_{efflux, app}(B\text{-}A)$ are the differences between P_{PD} and P_{app} in each direction that can be attributed to active transport, in this case, apparent permeability mediated by efflux. Although theoretically P_{PD} is the same in both A-B and B-A directions with a purely passive mechanism, it often appears different under experimental conditions, with A-B generally higher than B-A (Tables 2-4).

Practically, however, P_{PD} is often difficult to obtain, particularly when multiple transporters are involved. Therefore, transporter substrate index (e.g. $TSI_{A\text{-}B,}$ $TSI_{B\text{-}A,}$ and TSI_{ER}) is introduced here to capture the changes of P_{app} and ER for individual transporters in the presence (i) and absence of specific inhibitors in Eqs. (4-6):

$$TSI_{A\text{-}B} = \frac{P^i_{app}(A-B) - P_{app}(A-B)}{P_{app}(A-B)} \bullet 100\% = [\frac{P^i_{app}(A-B)}{P_{app}(A-B)} - 1] \bullet 100\% \quad (4)$$

$$TSI_{B\text{-}A} = \frac{P_{app}(B-A) - P^i_{app}(B-A)}{P_{app}(B-A)} \bullet 100\% = [1 - \frac{P^i_{app}(B-A)}{P_{app}(B-A)}] \bullet 100\% \quad (5)$$

$$TSI_{ER} = \frac{ER - ER^i}{ER} \bullet 100\% = [1 - \frac{ER^i}{ER}] \bullet 100\% \qquad (6)$$

10

Where P^i_{app}(A-B), P^i_{app}(B-A) and ER^i are P_{app}(A-B), P_{app}(B-A) and ER measured in the presence of a specific transporter inhibitor. The foundation of using TSIs to capture efflux activity is further supported by the three compartment kinetic model (Kalvass and Pollack, 2007). For instance, when efflux is completely inhibited, TSI_{A-B} bears conceptual similarity to Kalvass and Pollack's kinetic efflux ratio term which is proportional to efflux activity.

Importantly, TSIs allow more flexibility when efflux is not completely inhibited. First, they can be applied to NCEs involving multiple efflux transporters, where it is difficult to determine the true P_{PD} values by inhibiting all efflux processes.

Second, individual TSI can be quantified for each transporter impacting an NCE based on the extent of transporter-substrate interaction. The normalization of the TSI change in response to inhibition of each transporter allows for assessing the transporter specificity of an NCE and also flagging the potential for transporter-related DDI risk. In this report, TSIs were used for substrate classification and estimated efflux impact on *in vivo* absorption. TSI_{ER}, which characterizes the permeability change in both absorptive and secretory directions, was further proposed to rank individual transporters for their *in vivo* influence on exposure and DDI risk (see Results and Discussion).

Finally, in the cases where P_{PD}(A-B) could be obtained, the modified absorption quotient (AQ) was used in Eq. 7 (Troutman and Thakker 2003a):

$$AQ = \frac{P_{efflux, app}(A\text{-}B)}{P_{PD}(A\text{-}B)} = \frac{P_{PD}(A-B) - P_{app}(A-B)}{P_{PD}(A-B)} = 1 - \frac{P_{app}(A-B)}{P_{PD}(A-B)} \tag{7}$$

11

AQ provides a quantitative tool, especially for comparing a series of NCEs where a single transporter may dominate the transport mechanism (e.g. P-gp). Because our focus is on absorptive permeability, from this point forward $P_{efflux, app}$ and P_{PD} refer to apparent permeability mediated by efflux and passive diffusion in the A-B direction, unless specified otherwise.

DMD #34629

Results

Four-zone graphical model estimates efflux impact on absorption.

The absorptive transport [P_{app}(A-B)] in bi-directional cell-based assays is often used to predict human intestinal absorption (fraction absorbed, FA). To elucidate the relationship between efflux and P_{app}(A-B) as well as the impact of efflux on human intestinal absorption, P_{app}(A-B) was plotted against ER (log-log scale) for 63 structurally diverse marketed drugs which are reported transporter substrates (Fig. 1). Drugs were shaded by human FA in the figure. Overall, with increasing ER, P_{app}(A-B) and FA tended to decline, indicating efflux could pose a barrier to absorptive permeability, and consequently to intestinal absorption. The same trend was observed in a larger data set of 700 Novartis drug discovery NCEs (data not shown). Compounds were then quantitatively grouped into four zones based on the interplay among P_{app}, ER and FA, giving rise to the "four-zone graphical model". Drugs in zone 1 [P_{app}(A-B) ≥ 5 nm/s and ER <2] generally showed superior absorption (human FA 75-100%) and *in vitro-in vivo* correlation (IVIVC). Zone 2 [P_{app}(A-B) ≤ 5 nm/s and ER ≤ 2] was populated by few drugs with distinctive FA where *in vitro* permeability and *in vivo* absorption appeared to be largely governed by passive permeability. In zone 3 [P_{app}(A-B) ≥ 1.8 nm/s and ER ≥ 2], the magnitude (ER up to 10) and impact of efflux transport appeared limited as the *in vitro* permeability and intestinal absorption (FA 50-100%) remained adequate. The majority of drugs in zone 4 exhibited FA less than 50% as a result of low to moderate permeability [P_{app}(A-B) ≤ 1.8 nm/s] and significant efflux (ER: 2-30; for NCEs, ER was as high as 55). By dissecting the passive and active transport of the drugs (Eq. 2-3), we visualize an average P_{PD} of 12.8, 3.9, 11.2 and 2.6 nm/s from zone 1 to 4, while efflux

13

transporters counter-transported 29%, 41%, 54% and 63% of total passive permeability ($P_{efflux, app}$/P_{PD}) accordingly. The binning of P_{PD} follows P_{app} with 1 and 5 nm/s as the low and high permeability boundary. The four-zone graphical model proposed in the current work appeared useful in quickly screening out the potential poorly-absorbed NCEs. Importantly, it highlighted mainly zone 4 NCEs for further mechanistic studies to determine the role of P_{PD} and efflux activity when dealing with transporter-related optimization.

TSI substrate classification.

As shown in Fig. 1, efflux transporters distinctively attenuated *in vitro* absorptive permeability and in turn intestinal absorption. Therefore, it is imperative to quantitatively assess the contribution of efflux transport ($P_{efflux, app}$) to the overall drug permeation process (P_{PD}) (Eq. 2-3). This may be accomplished by saturating the efflux transporters (i.e. using escalated drug doses) or by inhibiting them to reduce the ER towards unity. The latter can also help identify the responsible transporter(s). Here, considering the critical role each plays in intestinal absorption, P-gp-, MRP2- and BCRP-mediated transport was studied in Caco-2 inhibition assay. For some, efflux transporter activities might be further confirmed by secondary transporter-transfected MDCK cell models or transporter-ATPase assays. The quantitative terms, $TSI_{A-B,}$ TSI_{B-A} and TSI_{ER}, were introduced to capture transporter activity change after inhibition and to determine substrate classification Eqs. (4-6). A combination of $TSI_{ER} \geq 25\%$ and TSI_{A-B} or TSI_{B-A} $\geq 25\%$ distinguished between substrates and non-substrates (Table 1). Due to the asymmetric kinetic effects of efflux transporters in absorptive and secretory transport (Troutman et al., 2003b; Kalvass and Pollack 2007), a substrate may display either

increased P_{app}(A-B), decreased P_{app}(B-A), or both after inhibition. Two underlying considerations for the criteria were 1) typically P_{app}(A-B) and P_{app}(B-A) fluctuated less than ±20% within a plate (data not shown); 2) using above criteria, all non-substrates and 91-100% of substrates were correctly identified for each transporter as reported in literature or in agreement with secondary assay results. Further, TSI_{ER} ≥50% differentiated a substrate as majorly versus partially transported by a specific transporter. This was based on the observation that compounds with significant *in vivo* oral absorption improvement upon blockage of a specific efflux transporter often had *in vitro* TSI_{ER} over 50% (Fig. 3). Specifically, published pharmacokinetic data from transporter knock-out (KO) mice compared to wild-type (WT) mice following oral dosing or *in situ* intestinal perfusion were examined (literature references for in vivo KO/WT mice and in situ perfusion data given in the footnote of Tables 2-3). Available AUC exposure or plasma concentration KO/WT ratios for mdr1 or Bcrp1, the murine homologues of MDR1 and BCRP, are presented in Tables 2-3. As shown in Fig. 3, a two-fold or greater ratio for either transporter was consistent with TSI_{ER} ≥50%. It should be noted that a substrate could have more than one partial or major transporter.

P-gp, MRP2 and BCRP substrate characterization.

P-gp. Sixty marketed drugs containing both P-gp substrates and non-substrates were selected for the test set of 1 µM LY335979 mediated P-gp inhibition (Table 2). Among them, 91% of substrates and 100% of non-substrates were correctly identified. Of note, the 9% false negative substrates, e.g. verapamil and nicardipine, resulted from high permeability or transporter saturation (Polli et al., 2001). Indeed, these would not be flagged as efflux in the standard bi-directional assay as their ER was near unity prior to

inhibition. Nor do they have a low absorption concern. For compounds transported majorly by P-gp such as colchicine, the ER decreased to ≤ 1, indicating the P-gp mediated efflux was completely abolished by the inhibitor. For others like vinblastine, ER remained above 2 after inhibition, suggesting involvement of additional transporters such as MRP2. Partially transported substrates such as sulindac showed a moderate TSI_{ER} of 29 for P-gp, while also indicated to be a major substrate for MRP2 (TSI_{ER}=60, Table 4). In contrast, non-substrates lacked change in TSIs, as observed for furosemide and fluvastatin, major substrates for both BCRP and MRP2.

BCRP. Ninety-four percent of BCRP substrates and 100% of non-substrates were correctly identified following inhibition by 1 μM Ko143 (Table 3). Metolazone, the only false negative BCRP substrate using TSIs, was confirmed as a substrate by in-house MDCK-Bcrp model (ER reduced from 5.1 to 1.4 following Ko143 inhibition).

MRP2. MK571 was reported to modulate multiple transporters including MRPs, P-gp and BCRP with distinctive potencies (IC_{50}s are 10, 26 and 50 μM, respectively) (Matsson et al 2009). Therefore, MK571 was used at low inhibitory concentration (10 μM) to distinguish MRPs inhibition from other transporters. Indeed, the efflux transport of colchicine (a P-gp-specific substrate, Table 2), nitrofurantoin (a BCRP-specific substrate, Table 3) and erythromycin (a major substrate for both P-gp and BCRP) were not affected under the current condition (Table 4). As the MK571 is less specific toward MRP2 than LY335979 and Ko143 against P-gp and BCRP respectively, it is best practice to characterize MRP2 after P-gp and BCRP inhibition studies. This study's results indicated a variety of drugs can be transported by MRP2 (Table 4). While some compounds were classified as substrates by an increase in P_{app}(A-B), the TSI_{ER} of others was mainly due to

the decrease of P_{app}(B-A). This suggested that by removing MRP2 activity, the absorption of compounds like dipyridamole would likely be improved, while the intestinal excretion of valsartan might be reduced. The classification of MRP2 substrates and non-substrates fully agreed with literature. The in-house MRP2 ATPase assay results also indicated substrates can activate MRP2, while non-substrates failed to do so.

Although not all substrates were tested against the three transporters in the current study, many showed greatly overlapped transporter substrate specificity. Daunorubicin, etoposide, teniposide and topotecan were transported by all three to different extent. Colchicine was solely transported by P-gp. BCRP was specifically responsible for norfloxacin. No compound in this test set was found only transported by MRP2. Interestingly, substrates often displayed distinctive response in absorptive and secretory directions. This was illustrated not only by the response of different compounds to the same inhibitor as mentioned above, but by the same compound's response to different inhibitors. For instance, daunorubicin was the major substrate of both P-gp and MRP2. However, the underlying mechanism appeared different as the reduction of secretory transport (TSI_{B-A}) was the main contributor of TSI_{ER} change for P-gp, while for MRP2 change was primarily attributed to the increase of TSI_{A-B}. Whether the reason is due to the involvement of multiple transporters or different substrate binding sites as well as the inhibition mechanisms requires further investigation.

Quantification and physiochemical properties of efflux attenuating absorptive transport.

Following the above substrate characterization, a subset of P-gp, MRP2 or BCRP substrates had ER ≤ 2 after inhibition, allowing for determination of P_{PD}. These 47

compounds were selected to further investigate the interplay of P_{app}(A-B), P_{PD}, and $P_{efflux, app}$ using AQ (Eq. 7). For a few compounds, more than one specific inhibitor reduced the ER sufficiently, resulting in multiple AQ values. In these cases the highest AQ value was used. In Fig. 2, compounds grouped in three bands based on P_{PD}, where the boundaries aligned with P_{app}(A-B) ranking values. A distinctive trendline (H, M or L) within each band was subsequently extrapolated, where higher AQ indicated greater attenuation of absorptive transport by efflux. Compounds with high P_{PD} and good oral absorption despite efflux activity (mostly zone 1 and 3) demonstrate a flatter regression line (H) with slope of -0.08. Compounds with medium P_{PD} and low to moderate oral absorption were less scattered along a steeper trendline (M) with slope of -0.38. The line (L) with slope of -0.5 was extrapolated from a smaller compound set with low P_{PD}. The majority of compounds along the trendlines M and L were from zone 4. Since the X-intercept reflected when P_{app}(A-B) equaled P_{PD} of each trendline according to Eq. (7), the compounds clustered around the H, M, L trendlines have average P_{PD} around 12.3, 2.6 and 1 nm/s, respectively.

Theoretically, the Y-intercept of each line should equal AQ of 1, where absorptive P_{PD} was counteracted by dominant efflux and P_{app}(A-B) reaches detection limits. While the intercepts for trendlines H and M were close to 1, the trendline L intercepted the Y-axis at 0.5. It is likely that the low passive permeability effectively limited the substrates' access to the trans-membrane transporters, resulting in a low $P_{efflux, app}$ that restricted $P_{efflux, app}$ /P_{PD} from approaching 1. A similar observation was noted for P-gp substrates that were outliers from a linear relationship between AQ and $\log P_{app}$(A-B) (Varma et al. 2005). Indeed, Troutman et al. (2003a) originally reported a parabolic relationship between AQ

and P_{PD}, suggesting that moderately permeable P-gp substrates were most susceptible to

P-gp-mediated efflux. Here, no distinction was observed between P-gp, BCRP or MRP2

related transport activities.

Discussion

Four-zone model to quickly filter problematic efflux transporter substrates.

While GI drug transport involves multiple mechanisms, passive diffusion is often the first target for optimization. The Caco-2 four-zone graphical model captures the contribution of both P_{PD} and $P_{efflux,\ app}$ and determines a compound's possible range of intestinal absorption. It is clear that zone 1 compounds are preferred over others. For zone 2 NCEs, optimization may focus on P_{PD} as the percentage of $P_{efflux,\ app}$ remained comparatively low. Zone 3 compounds, despite higher percentage of $P_{efflux,\ app}$, would be less of a concern in permeability-limited oral absorption due to high P_{PD} and possible transporter saturation at the intestinal level (Stenberg et al., 2002). However, together with zone 4, they are more susceptible to transporter mediated DDI due to the substantial involvement of efflux in the overall permeability. Attention should be focused on zone 4 compounds where P_{PD} and $P_{efflux,\ app}$ became comparable. Mechanistic studies (inhibition or dose escalation) were necessary to determine whether efflux, $P_{PD,}$ or both limit absorption in zone 4. The dominant contribution of passive mechanism in overall drug transport observed in the zone separation is consistent with the fact that the partitioning into lipid membrane is considered the rate limiting step for substrate interaction with transporters (Seelig and Landwojtowiez, 2000).

Indeed, more Novartis NCEs were observed in zone 4 compared to marketed drugs. Therefore challenges should be anticipated for NCEs with poor physicochemical properties. Moreover, the boundary for zone 3 and 4 may change for different chemical series due to various solubility, dose, and therapeutic drug levels. The transporter expression in cells used to generate this model also influences zone boundaries. Ours

agreed with human jejunal biopsy rank on efflux transporters with BCRP > MRP2 > P-gp at day-21 (Hilgendorf et al., 2007).

Of note, Wu and Bennet (2005) considered the role of active transport (efflux and uptake) for drug disposition within the Biopharmaceutics Drug Disposition Classification System (BDDCS). While BDDCS recommended when transporters should be evaluated in drug absorption/elimination based on solubility, permeability and metabolism, the four-zone model is based on permeability, with a focus on efflux transporter impact on intestinal absorption. Given the different classification criteria, it is not surprising that a comparison of the two systems showed no obvious overlap between drugs assigned to zones 1-4 and BDDCS class (data not shown).

TSI applications.

TSIs are particularly useful in projecting individual transporter impact on oral absorption when multiple transporters are involved. For instance, TSI_{ER} measures the change of substrate transport in response to specific transporter inhibitors. When compared with available *in vivo* or *in situ* studies, substrates with $TSI_{ER} \geq 50$ often had a greater than two-fold increase in AUC or plasma concentration in gene KO over WT mice following oral dosing (Fig. 3). In contrast, when $TSI_{ER} < 50$, this increase often was mild or negligible. This observation provided the fundamental reason to separate major versus partial substrates (Table 1). Indeed, the degree of efflux inhibition needed to reverse efflux effect is related to the ER (Kalvass and Pollack 2007). Therefore, it is not surprising to see such a correlation between TSI_{ER} and *in vivo* transporter activity. Although few, there were exceptions, including vinblastine ($TSI_{ER}=88$, *mdr*1

$AUC_{KO}/AUC_{WT}=1.5$). It was possible that a great portion of drug was absorbed through duodenum where P-gp expression was minimal (Ogihara et al., 2006). Of note, AUC or plasma concentration ratio between KO and WT does not distinguish the transport across GI tract from other clearance processes. The *in vivo* dose and formulation are also different from *in vitro*. Therefore, a linear relationship between TSI_{ER} and exposure was not expected. Rather, TSI_{ER} flagged when a meaningful reduction in oral exposure was likely for a substrate mitigated by a specific transporter.

TSI_{ER} may also be used to address the overlapped substrate specificity by ranking the relative contribution of each transporter. For example, topotecan was found to be transported by BCRP (TSI_{ER}=76) and P-gp (TSI_{ER}=51). Correspondingly, the *bcrp1-/-* mice showed a 6-fold AUC increase over WT mice (Jonker et al. 2002), while the ratio was 2 in *mdr1a-/-* mice when dosing orally (Jonker et al. 2000). Similarly, sulfasalazine, a major substrate of BCRP (TSI_{ER}=62) but a non-substrate of P-gp (TSI_{ER}=5), was reported with a 111- and 1.3-fold increase of AUC in *bcrp1-/-* and *mdr1a-/-* mice, respectively (Zaher et al., 2006). It followed that TSI_{ER} could potentially be applied to absorption window design. The three studied transporters express differentially along the human intestine: P-gp level increases from proximal to distal, MRP2 does the opposite, while BCRP has highest expression in jejunum (Murakami et al., 2008). One may target or avoid drug delivery to intestinal regions based on the contribution of individual transporters as reflected by TSI_{ER}.

In addition, TSI_{ER} has potential application towards assessing DDI. Considering transporters' strategic distribution and broad substrate/inhibitor spectrum, safety concerns have been raised on transporter mediated DDI. Like CYP450 substrates, the risk largely

depends on the transporter specificity and degree of interaction. The exposure of a substrate may be less susceptible to a single transporter modulator if there is compensation by other pathways. For instance, the systemic exposure of digoxin (TSI_{ER}=87) is predominantly influenced by specific P-gp inhibitors (Fenner et al., 2009). In contrast, the AUC increase of topotecan was greater with GF120918, an inhibitor of both Bcrp1 and mdr1 (9- versus 6- and 2-fold for individual transporters, Jonker et al. 2000). The clinical relevance of transporter-mediated DDI for a wide range of drugs is still under investigation. However, TSI_{ER} ranking across the transporters may serve as a potential tool to assess DDI risk.

The AQ-P_{app}(A-B) chart.

In the AQ-P_{app}(A-B) chart (Fig. 2), structurally unrelated substrates grouped by their individual P_{PD} along three trendlines, which illustrated the fundamental influence of physicochemical properties on absorptive transport. For instance, MW and PSA, partially accounting for membrane permeation, increased on average from the trendlines H to L. Additional work with a larger data set is ongoing to discriminate the compound trendlines further using pharmacophore and statistical modeling. Ultimately, without further mechanistic experiments, an AQ model may allow estimation of P_{PD} and the highest AQ for NCEs using only P_{app}(A-B) by correctly projecting compounds onto each line based on their physicochemical properties.

Another important application of the AQ-P_{app}(A-B) chart is to distinguish efflux from low permeability issues and prioritize compounds based on the impact of the two on absorption. For instance, a series of mostly zone 4 Novartis compounds had low to moderate oral exposure. From mechanistic studies, they were identified as major

substrates of P-gp and subsequently projected onto the AQ-P_{app}(A-B) chart (Fig. 2). The emerging three groups illustrated chemistry strategy. Compounds on the H band were limited by efflux, however exposure can be improved if efflux activity was modulated by *in vivo* P-gp saturation (low Km_{app}), or co-administration of P-gp inhibitors (high AQ) (Kuppens et al., 2005). For those compounds along the M band, oral absorption would be limited by sub-optimal passive permeability and efflux. Because the majority of compounds projected along this line, line position could guide structure-activity relationships (SAR). Compounds along the L band were subject to poor passive permeability, with or without efflux activity. In this case the AQ-P_{app}(A-B) chart quickly alerted the project that structural modification was needed in order to improve physicochemical properties favoring passive permeability.

In conclusion, we have suggested a sequential strategy to assess potential efflux attenuation of permeability and absorption for NCEs in early discovery. By using the Caco-2 four-zone graphical model, compounds are filtered for further mechanistic studies, where one can be alerted to compounds with efflux liability or opportunities for improved IVIVC. The novel TSI parameters allow (1) classifying major roles of multiple transporter(s) on exposure, and (2) identifying substrate specificity for targeted delivery or potential transporter-mediated DDI risk. Mapping P_{app}(A-B) versus AQ provided a quantitative tool, enabling optimization of physicochemical properties and establishment of transporter SAR. The rational understanding of P_{PD} and P_{efflux} interplay enables quantitative prediction of efflux-attenuated GI absorption and offers valuable guidance for lead candidate selection and optimization.

24

DMD #34629

Acknowledgements

DMD #34629

Authorship Contributions

Participated in research design: Lin, Skolnik, Chen, Wang

Conducted experiments: Lin, Skolnik, Chen

Contributed new reagents or analytic tools: Lin, Skolnik, Chen, Wang

Performed data analysis: Lin, Skolnik, Chen, Wang

Wrote or contributed to the writing of the manuscript: Lin, Skolnik, Wang

References

Adachi Y, Suzuki H, Sugiyama Y (2003) Quantitative Evaluation of the Function of Small Intestinal P-Glycoprotein: Comparative Studies Between *in Situ* and *in Vitro. Pharm. Res.,* **20**: 1163-1169.

Allen JD, van Loevezijn A, Lakhai JM, van der Valk M, van Tellingen O, Reid G, Schellens JH, Koomen GJ, Schinkel AH (2002) Potent and specific inhibition of the breast cancer resistance protein multidrug transporter in vitro and in mouse intestine by a novel analogue of fumitremorgin C. *Mol Cancer Ther.* **1**:417-425.

Bonhomme-Faivre L, Benyamina A, Reynaud M, Farinotti R, Abbara C (2008) Disposition of Delta 9-tetrahydrocannabinol in CFI mice deficient in mdr1a P-glycoprotein. *Addict Biol.* **13**:295-300.

Chen C, Liu X, Smith BJ (2003) Utility of Mdr1-gene deficient mice in assessing the impact of P-glycoprotein on pharmacokinetics and pharmacodynamics in drug discovery and development. *Curr Drug Metab* **4** : 272 -291.

Chen C, Lin J, Smolarek T, Tremaine L (2007) P-glycoprotein Has Differential Effects on the Disposition of Statin Acid and Lactone Forms in *mdr1a/b* Knockout and Wild-Type Mice. *Drug Metab Dispos* **35**:1725-1729.

Choudhuri S, Klaassen CD (2006) Structure, Function, Expression, Genomic Organization,and Single Nucleotide Polymorphisms of Human ABCB1 (MDR1), ABCC (MRP), and ABCG2 (BCRP) Efflux Transporters. *Int J Toxicol* **25**:231–259.

Dantzig AH, Shepard RL, Cao J, Law KL, Ehlhardt WJ, Baughman TM, Bumol TF, Starling JJ (1996) Reversal of P-Glycoprotein-mediated Multidrug Resistance by a Potent Cyclopropyldibenzosuberane Modulator, LY335979. *Cancer Res.* **56**: 4171-4179.

Dautrey S, Felice K, Petiet A, Lacour B, Carbon C, Farinotti R (1999)   Active intestinal elimination of ciprofloxacin in rats: modulation by different substrates.   *Br J Pharmacol* **127**: 1728-1734.

Eberl S, Renner B, Neubert A, Reisig M, Bachmakov I, König J, Dörje F, Mürdter TE, Ackermann A, Dormann H, Gassmann KG, Hahn EG, Zierhut S, Brune K, Fromm MF (2007) Role of P-Glycoprotein Inhibition for Drug Interactions: Evidence from In Vitro and Pharmacoepidemiological Studies. *Clin Pharmacokinet* **46**:1039-1049.

Fenner KS, Troutman MD, Kempshall S, Cook JA, Ware JA, Smith DA, Lee CA (2009) Drug-drug interactions mediated through P-glycoprotein: clinical relevance and in vitro-in vivo correlation using digoxin as a probe drug. *Clin Pharmacol Ther.* **85**:173-181.

Gekeler V, Ise W, Sanders KH, Ulrich WR, Beck J (1995) The leukotriene LTD4 receptor antagonist MK571 specifically modulates MRP associated multidrug resistance. *Biochem Biophys Res Commun.* **208**:345-352.

Giacomini KM, Sugiyama Y (2006) Membrane transporters and drug response, in *The Pharmacological Basis of Therapeutic* pp41–70, McGraw-Hill, New York.

Giri N, Shaik N, Pan G, Terasaki T, Mukai C, Kitagaki S, Miyakoshi N, Elmquist WF (2008) Investigation of the role of breast cancer resistance protein (Bcrp/Abcg2) on pharmacokinetics and central nervous system penetration of abacavir and zidovudine in the mouse. *Drug Metab Dispos.* **36**:1476-1484.

Hilgendorf C, Ahlin G, Seithel A, Artursson P, Ungell AL, Karlsson J (2007) Expression of thirty-six drug transporter genes in human intestine, liver, kidney, and organotypic cell lines. *Drug Metab Dispos.* **35**:1333-40.

Igel S, Drescher S, Mürdter T, Hofmann U, Heinkele G, Tegude H, Glaeser H, Brenner SS, Somogyi AA, Omari T, Schäfer C, Eichelbaum M, Fromm MF (2007) Increased Absorption of Digoxin from the Human Jejunum Due to Inhibition of Intestinal Transporter-Mediated Efflux. *Clin Pharmacokinet* **46**: 777-785.

Jonker JW, Smit JW, Brinkhuis RF, Maliepaard M, Beijnen JH, Schellens JHM, Schinkel AH (2000) Role of Breast Cancer Resistance Protein in the Bioavailability and Fetal Penetration of Topotecan. *J Natl Cancer Inst.* **92**: 1651-1656.

Jonker JW, Buitelaar M, Wagenaar E, Van Der Valk MA, Scheffer GL, Scheper RJ, Plosch T, Kuipers F, Elferink RP, Rosing H, Beijnen JH, Schinkel AH (2002) The breast cancer resistance protein protects against a major chlorophyll-derived dietary phototoxin and protoporphyria. *Proc Natl Acad Sci* **99**:15649-15654.

Kalvass JC, Pollack GM (2007) Kinetic considerations for the quantitative assessment of efflux activity and inhibition: implications for understanding and predicting the effects of efflux inhibition. *Pharm Res.* **24**:265-276.

Kuppens IE, Bosch TM, van Maanen MJ, Rosing H, Fitzpatrick A, Beijnen JH, Schellens JH (2005) Oral bioavailability of docetaxel in combination with OC144-093 (ONT-093). *Cancer Chemother Pharmacol.* **55**:72-78.

Mahar Doan KM, Humphreys JE, Webster LO, Wring SA, Shampine LJ, Serabjit-Singh CJ, Adkison KK, Polli JW (2002) Passive permeability and P-glycoprotein-mediated efflux differentiate central nervous system (CNS) and non-CNS marketed drugs. *J Pharmacol Exp Ther.* **303**:1029-1037.

Mahony C, Wolfram KM, Nash PV, Bjornsson TD (1983) Kinetics and metabolism of sulfinpyrazone. *Clin Pharmacol Ther* **33:**491-497.

Matsson P, Pedersen JM, Norinder U, Bergström CA, Artursson P (2009) Identification of novel specific and general inhibitors of the three major human ATP-binding cassette transporters P-gp, BCRP and MRP2 among registered drugs. *Pharm Res.* **26**:1816-1831.

Merino G, Jonker JW, Wagenaar E, van Herwaarden AE, Schinkel AH (2005) The breast cancer resistance protein (BCRP/ABCG2) affects pharmacokinetics, hepatobiliary excretion, and milk secretion of the antibiotic nitrofurantoin. *Mol Pharmacol.* **67**:1758-1764.

Merino G, Alvarez AI, Pulido MM, Molina AJ, Schinkel AH, Prieto JG (2006) Breast cancer resistance protein (BCRP/ABCG2) transports fluoroquinolone antibiotics and affects their oral availability, pharmacokinetics, and milk secretion. *Drug Metab Dispos.* **34**:690-695.

Mimeault M, Hauke R, Batra SK (2008) Recent advances on the molecular mechanisms involved in the drug resistance of cancer cells and novel targeting therapies. *Clin Pharmacol Ther* **83**:673-691.

Murakami T, Takano M (2008) Intestinal efflux transporters and drug absorption. *Expert Opin drug Metab Toxicol.* **4**: 923-939.

Ogihara T, Kamiya M, Ozawa M, Fujita T, Yamamoto A, Yamashita S, Ohnishi S, Isomura Y (2006) What kinds of substrates show P-glycoprotein-dependent intestinal absorption? Comparison of verapamil with vinblastine. *Drug Metab Pharmacokinet.* **21**:238-244.

Oostendorp RL, Buckle T, Beijnen JH, van Tellingen O, Schellens JH (2009) The effect of P-gp (Mdr1a/1b), BCRP (Bcrp1) and P-gp/BCRP inhibitors on the in vivo absorption, distribution, metabolism and excretion of imatinib. *Invest New Drugs.* **27**:31-40.

Polli JW, Wring SA, Humphreys JE, Huang L, Morgan JB, Webster LO, Serabjit-Singh CJ (2001) Rational use of in vitro P-glycoprotein assays in drug discovery. *J Pharmacol Exp Ther* **299**:620–628.

Schellens JH, Creemers GJ, Beijnen JH, Rosing H, de Boer-Dennert M, McDonald M, Davies B, Verweij J (1996) Bioavailability and pharmacokinetics of oral topotecan: a new topoisomerase I inhibitor. *Br J Cancer.* **73**:1268-1271.

Seelig A, Landwojtowicz E (2000) Structure–activity relationship of P-glycoprotein substrates and modifiers. *Euro J of Pharm Sci.* **12**:31–40.

Skolnik S, Lin X, Wang J, Chen X, He T, Zhang B (2010) Towards prediction of in vivo intestinal absorption using a 96-well Caco-2 assay. *J Pharm Sci.* **99**:3246-65.

DMD #34629

Stenberg P, Bergstrom CA, Luthman K, Artursson P (2002) Theoretical predictions of drug absorption in drug discovery and development. *Clin. Pharmacokine*; **41**: 877-899.

Troutman MD, Thakker DR (2003a) Novel experimental parameters to quantify the modulation of absorptive and secretory transport of compounds by P-glycoprotein in cell culture models of intestinal epithelium. *Pharm Res* **20**:1210-1224.

Troutman MD, Thakker DR (2003b) Efflux Ratio Cannot Assess P-Glycoprotein-Mediated Attenuation of Absorptive Transport: Asymmetric Effect of P-Glycoprotein on Absorptive and Secretory Transport across Caco-2 Cell Monolayers. *Pharm. Res,* **20:** 1200-1208.

van de Waterbeemd H, Camenisch G, Folkers G, Chretien JR, Raevsky OA (1998) Estimation of blood-brain barrier crossing of drugs using molecular size and shape, and H-bonding descriptors. *J Drug Target* **6**:151-165.

Varma MV, Sateesh K, Panchagnula R (2005) Functional role of P-glycoprotein in limiting intestinal absorption of drugs: contribution of passive permeability to P-glycoprotein mediated efflux transport. *Mol Pharm* **2**:12-21.

Wu CY, Benet LZ (2005) Predicting drug disposition via application of BCS: transport/absorption/ elimination interplay and development of a biopharmaceutics drug disposition classification system. *Pharm Res.* **22**:11-23.

DMD #34629

Zaher H, Khan AA, Palandra J, Brayman TG, Yu L, Ware JA (2006)   Breast cancer resistance protein (Bcrp/abcg2) is a major determinant of sulfasalazine absorption and elimination in the mouse.   *Mol Pharmaceutics* **3**: 55-61.

Zhou L, Schmidt K, Nelson FR, Zelesky V, Troutman MD, Feng B (2009) The Effect of Breast Cancer Resistance Protein and P-Glycoprotein on the Brain Penetration of Flavopiridol, Imatinib Mesylate (Gleevec), Prazosin, and 2-Methoxy-3-(4-(2-(5-methyl-2-phenyloxazol-4-yl)ethoxy)phenyl)propanoic   Acid   (PF-407288)   in   Mice. *Drug Metab Dispos* **37**: 946-955.

DMD #34629

Legends for Figures:

Figure 1. Four zone graphical model to estimate the efflux impact on intestinal absorption. Sixty-three reported or current assay identified substrates with human fraction absorbed (FA) were plotted using P_{app}(A-B) against ER in log-log scale. Substrates were ranked by FA (white: $\geq$ 75%, gray: 35-75%, black: $\leq$ 35%). Four zones were defined as follows: zone 1 [P_{app}(A-B) $\geq$5 nm/s and ER <2] where compounds have superior intestinal absorption and efflux will not be the limiting factor due to high passive permeability; zone 2 [(P_{app}(A-B) <5 nm/s and ER <2] where compounds can have various FA and passive permeability but not efflux is the major determinant; zone 3 [(P_{app}(A-B) $\geq$1.8 nm/s and ER $\geq$2] where the FA of compounds remains adequate because passive permeability is sufficiently high to overcome efflux; and zone 4 [(P_{app}(A-B) <1.8 nm/s and ER $\geq$2] where passive permeability and efflux become comparable, and mechanistic studies are required to understand the net outcome of the two competing processes. The data with ER <1 may result from potential involvement of uptake transporter(s) and/or asymmetrical passive permeability intrinsic to the current assay configuration (e.g. distinctive surface area and/or drug accessibility in the apical and basolateral sides).

Figure 2. Quantification of efflux attenuating absorptive transport using AQ and P_{app}(A-B) and subsequently applying AQ chart to evaluate efflux impact on oral absorption for NCEs. A subset of 47 marketed drugs with ER <2 after inhibition was chosen for the plot. Compounds were color coded by P_{PD} (white: high $\geq$5 nm/s; gray: medium 1-5 nm/s; black: low $\leq$1 nm/s). Compounds appeared to group into three bands

35

based on their P_{PD} (high: white; medium: grey; low: black). Distinct trendlines (H, M and L) were extrapolated from each band with R^2 of 0.45, 0.62 and 0.99 from H to L respectively. Compounds in zones 1-3 tended to cluster along trendline H, while zone 4 compounds were more distributed along trendlines M and L. The slopes were calculated using Excel linear fit with Y intercept forced through AQ=1 for lines H and M. The intercepts at X-axis were 12.3, 2.6, and 1.0 nm/s for trendlines H, M and L respectively. The average MW and PSA for compounds along each line were shown in parentheses. Subsequently, a series of zone 4 Novartis compounds from a single project were projected onto the AQ chart after P-gp inhibition study. Compounds along the trendline H had good passive permeability and low apparent K_m which favored adequate exposure. For compounds clustered along M or L lines, complete inhibition of efflux activity or dose escalation did not greatly improve their absorptive transport.

Figure 3. A comparison of TSI$_{ER}$ with the *in vivo* or *in situ* plasma AUC or concentration ratio from knock out (KO) versus wild type (WT) mice. Majority of compounds with TSI$_{ER}$ $\geq$50 had at least two-fold increase in previously published plasma AUC or concentration ratios (mdr1 or Bcrp1 KO versus WT), while this change was insignificant for those with TSI$_{ER}$<50. This suggests that TSI$_{ER}$ may help define major versus partial substrate based on the potential *in vivo* impact of the responsible transporter. (Literature references for KO and WT mice data given in the footnote of Tables 2-3.)

Tables

DMD #34629

Table 1. Classification criteria for transporter substrates.

	TSI_{ER}		TSI_{A-B} and TSI_{A-B}
Partial substrate	25%-50%	AND	$TSI_{PappA-B}$ and/or $TSI_{PappB-A} >= 25\%$
Major substrate	>=50%	AND	$TSI_{PappA-B}$ and/or $TSI_{PappB-A} >= 25\%$

Note: If either TSI_{ER} or $TSI_{Papp} < 25\%$, compounds are classified as non-substrate.

37

Table 2. P-gp substrate classification based on Caco-2 permeability in the presence and absence of 1μM LY335979. P_{app} values were presented as mean with CV% $\leq$15 in triplicate. Drugs were classified based on the criteria in Table 2.

Compound[a]	%FA[b]	P_{app}A-B nm/s	P_{app}B-A nm/s	ER (MDCK-MDR1 ER[c])	P_{app}A-B nm/s(i)[d]	P_{app}B-A nm/s(i)	ER(i)	TSI$_{PappA-B}$	TSI$_{PappB-A}$	TSI$_{ER}$	AQ	Plasma AUC or Concentration ratio (KO/WT)[e]
Major substrate												
Acebutolol	70	1.1	4.1	3.6	3.0	3.0	1.0	168	25	72	0.63	
ActinomycinD	5	0.8	13.0	15.9	2.3	9.3	4.0	182	28	75		
Amprenavir	70	8.0	27.0	3.4 (16)	19.2	14.9	0.8	139	45	77	0.58	1.3
Cetirizine	66	3.9	7.6	2.6	5.7	4.4	0.8	45	42	69	0.31	
Chloroquine	89	1.0	2.2	2.2	3.4	2.6	0.8	241	-20	65	0.71	
Clarithromycin	50	3.5	18.0	5.1	11.9	9.4	0.8	238	48	85	0.7	
Colchicine	44	1.3	7.2	5.6	2.9	2.4	0.8	120	67	85	0.55	
Daunorubicin	10	1.1	2.7	2.5	0.9	0.4	0.4	-16	86	83	-0.2	3.0*
Digoxin	68	1.1	8.5	7.5 (27)	5.0	5.0	1.0	339	41	87	0.77	2.4, 12*

38

Domperidone	93	5.7	16.1	2.8 (22)	11.0	8.2	0.7	93	49	74	0.48	2
Emetine	n/a	2.4	6.0	2.6	3.6	2.0	0.6	53	66	78	0.35	
Erythromycin	35	0.3	5.3	15.5	1.2	0.6	0.5	251	88	97	0.71	3.4
Etoposide	25	0.7	4.1	6.4 (11)	1.6	2.1	1.4	143	49	79	0.59	3.3*
Fexofenadine	n/a	1.2	2.3	2.0	1.7	1.0	0.6	46	57	70	0.32	4.6
Fluconazole	95	11.6	6.7	0.6	10.3	1.2	0.1	-11	83	81	-0.13	
Indinavir	63	2.4	22.8	9.7	15.2	12.6	0.8	546	45	91	0.85	2
Ivermectin	56	0.8	9.6	12.2	1.4	0.8	0.53	82	92	96	0.45	3.3
Labetalol	95	2.8	4.5	1.6	5.7	3.0	0.5	101	33	67	0.5	
Loperamide	40	5.8	7.6	1.3	10.0	4.5	0.5	73	40	66	0.42	2.0, 3.1*
Methylprednisolone	82	8.5	24.6	2.9	16.1	12.1	0.8	89	51	74	0.47	
Nelfinavir	3	0.7	1.7	2.5	0.8	0.6	0.7	25	65	72	0.2	4.8
Paclitaxel	6	0.8	8.4	10.1	3.7	4.7	1.3	348	44	87	0.78	6.0, 17*
Ritonavir	66	2.1	9.2	4.5	9.7	6.4	0.7	370	31	85	0.79	4.7*
Saquinavir	4	0.4	8.6	24.9	2.4	3.2	1.3	595	63	95	0.86	6.5
Sumatriptan	57	1.5	2.2	1.4	3.2	1.5	0.5	107	32	67	0.52	

Tacrolimus	25	1.0	3.6	3.5	1.0	0.7	0.7	-1	81	80	-0.01	8.2
Teniposide	0	0.9	9.2	9.8	2.0	4.4	2.1	117	53	78		
Topotecan	30	0.7	18.7	26.0	1.3	17.2	13.1	82	8	50		2.3
Trifluoperazine	16	0.5	1.0	1.9	1.3	1.1	0.9	144	-16	53	0.59	
Vinblastine	5	0.7	11.9	16.5	3.2	6.5	2.0	340	46	88	0.77	1.5, 0.7-3.9*
Vinorelbine	45	1.4	8.5	5.9	3.0	3.0	1.0	108	65	83	0.52	
Partial substrate												
Cimetidine	60	1.4	4.8	3.5	2.4	4.3	1.8	74	11	49	0.42	0.95*
Ciprofloxacin	69	2.4	8.4	3.5	2.1	4.1	2.0	-15	51	42	-0.18	1.6*
Cyclosporin A	40	1.0	5.8	5.6	2.5	8.1	3.2	144	-41	42		0.6-0.9
Diltiazem	92	12.0	8.3	0.7 (0.8)	15.0	6.6	0.4	25	20	36	0.2	
Dipyridamole	66	5.1	18.7	3.7	8.9	18.5	2.1	75	1	44		
Fluoxetine	70	2.1	1.3	0.6	2.8	1.0	0.4	31	20	39	0.24	0.97
Imatinib	67	4.1	5.2	1.3 (3.1)	5.8	3.8	0.7	43	27	49	0.3	0.8
Irinotecan	n/a	1.2	5.1	4.4	1.5	4.1	2.7	29	21	38		
Metolazone	64	2.9	11.3	3.8	2.7	5.8	2.1	-7	48	44		

Olsalazine	2.3	0.9	3.1	3.7	0.9	1.7	1.9	7	44	48	0.07	
Prazosin	100	9.0	20.5	2.3	13.2	21.0	1.6	47	-2	30	0.32	1.2
Sulindac	90	3.7	13.5	3.6	5.2	13.3	2.6	39	2	29		
Trimethoprim	97	15.9	11.2	0.7	26.8	11.6	0.4	68	-4	38	0.41	
Valsartan	25	0.4	1.7	4.1	0.5	1.5	2.9	25	13	30		
Vincristine	<10	0.4	4.7	13.2	0.4	3.2	8.6	3	33	35		
Non-substrate												
Amrinone	93	7.5	20.4	2.7	4.3	14.4	3.3	-43	30	-23		
Fluvastatin	98	1.9	20.6	10.9(4.9)	1.0	12.4	12.3	-47	40	-13		
Furosemide	61	0.7	6.6	9.1 (3.1)	1.1	9.4	8.3	55	-43	8		
Haloperidol	60	4.1	1.8	0.4	7.1	2.9	0.4	72	-61	6		
HBED	5	0.02	0.04	2.1	0.02	0.04	2.0	7	-5	2		
Ketoconazole[#]	90	18.0	5.1	0.3	26.2	6.7	0.3	46	-31	10		1.6
Mitoxantrone	85	26.3	12.5	0.5	14.3	7.9	0.6	-46	37	-16		
Naloxone[#]	91	21.5	10.3	0.5 (0.7)	21.5	10.5	0.5	0	-2	-2		
Nicardipine[#]	100	5.0	2.6	0.5	4.2	2.2	0.5	-16	16	0		

Norfloxacin	40	1.9	3.3	1.7	2.9	4.9	1.7	47	-48	0	
Reserpine[#]	50	3.6	2.3	0.6	3.9	2.7	0.7	10	-16	-5	1.2
Sulfasalazine	13	0.4	14.7	34.0	0.5	15.7	32.2	13	-7	5	1.3
Sulfinpyrazone	85	1.2	8.4	6.9	1.2	10.9	9.0	-1	-30	-31	
Verapamil[#]	100	9.0	4.6	0.5	8.1	4.3	0.5	-10	6	-4	

(i) indicates the presence of LY335979 1 μM.

[a] P-gp substrate and non-substrate ref. source: Polli et al., 2001; Mahar Doan et al., 2002; Varma et al., 2005; Choudhuri et al., 2006.

[b] Human FA_{exp} ref. source: Skolnik et al,. 2010; Mahony et al.,1983; Schellens et al., 1996 and Thomson MICROMEDEX database.

[c] ER from MDCK-MDR1 bi-directional assay was given in parentheses, where ER ≥ 5 is considered as the boundary for substrates. Note: similar to Caco-2, the

ER is also subject to the limitations of bi-directional assay approach.

[d] $P_{PD}(A-B)$ equals $P_{app}(A-B)(i)$ when $ER(i) \leq 2$.

[e] Pharmacokinetic data following p.o. administration from *mdr1* knock out (KO) versus wild type (WT) mice. The *in vivo* ref. source: Ogihara et al., 2006; Chen

et al., 2003 and 2007; Zaher et al., 2006; Bonhomme-Faivre et al., 2008. *in situ* intestinal perfusion ref. source: Dautrey et al., 1999; Adachi et al., 2003.

[#] False negative substrate

Table 3. **BCRP substrate classification based on Caco-2 permeability in the presence and absence of Ko143.** P_{app} values were presented as mean with CV% $\leq$15 in triplicate. Drugs were classified based on the criteria in Table 2.

Compound[a]	%FA	P_{app}A-B nm/s	P_{app}B-A nm/s	ER (MDCK-Bcrp ER[b])	P_{app}A-B nm/s(i)	P_{app}B-A nm/s(i)	ER(i)	TSI$_{PappA-B}$	TSI$_{PappB-A}$	TSI$_{ER}$	AQ	Plasma AUC or Concentration ratio (KO/WT)[c]
Major substrate												
Cerivastatin	98	5.4	5.0	0.9	8.8	3.1	0.4	64	37	62	0.4	
Erythromycin	35	0.4	3.0	8.1 (8.5)	0.6	1.7	2.7	72	43	67		
Etoposide	25	0.5	6.8	12.7(9.7)	1.1	3.4	3.1	106	49	75		
Fluvastatin	98	2.1	10.3	4.9	4.7	3.9	0.8	123	63	83	0.6	
Furosemide	61	0.6	9.7	17.5	1.6	4.5	2.8	190	53	84		
Irinotecan	na	1.4	5.0	3.7	2.3	3.9	1.7	66	23	54	0.4	
Nitrofurantoin	100	0.8	18.8	24.1	4.0	7.2	1.8	409	61	92	0.8	4
Norfloxacin	40	1.9	5.6	3.0	2.7	3.2	1.2	44	43	61	0.3	
Rosuvastatin	20	0.5	7.5	15.9	0.9	6.8	7.9	82	10	50		

43

Compound[a]	%FA	P_{app}A-B nm/s	P_{app}B-A nm/s	ER (MDCK-Bcrp ER[b])	P_{app}A-B nm/s(i)	P_{app}B-A nm/s(i)	ER(i)	$TSI_{PappA-B}$	$TSI_{PappB-A}$	TSI_{ER}	AQ	Plasma AUC or Concentration ratio (KO/WT)[c]
Sulfasalazine	13	0.8	13.4	16.9	1.5	9.7	6.4	91	28	62		111
Teniposide	0	0.8	8.8	10.8	1.5	8.2	5.4	84	8	50		
Topotecan	30	1.0	7.1	6.9 (2.4)	2.4	3.9	1.6	130	45	76	0.6	6
Partial substrate												
Ciprofloxacin	69	2.5	5.2	2.1	2.8	3.9	1.4	12	26	34	0.1	2
Daunorubicin	10	0.4	2.1	4.9	0.5	1.6	3.3	9	27	33		
Imatinib	67	3.7	6.0	1.6	5.9	5.6	1.0	59	6	41	0.4	1.3
Prazosin	100	6.2	11.1	1.8	6.7	8.0	1.2	9	28	34	0.1	
Zidovudine	90	6.7	9.6	1.4	7.4	7.1	1.0	10	26	33	0.1	0.97
Non-substrate												
Actinomycin D	5	0.7	4.5	6.4	0.4	8.2	5.4	115	-82	15		
Colchicine	44	0.9	6.6	7.6	0.9	5.6	6.4	1	16	16		

44

Compound[a]	%FA	P_{app}A-B nm/s	P_{app}B-A nm/s	ER (MDCK-Bcrp ER[b])	P_{app}A-B nm/s(i)	P_{app}B-A nm/s(i)	ER(i)	$TSI_{PappA-B}$	$TSI_{PappB-A}$	TSI_{ER}	AQ	Plasma AUC or Concentration ratio (KO/WT)[c]
Digoxin	68	0.9	12.6	14.6 (1.3)	0.9	10.4	11.8	2	17	19		
Metolazone[#]	64	2.9	9.6	3.3 (5.1)	3.4	8.2	2.4	16	15	27		
Paclitaxel	6	0.4	9.1	21.4	0.3	8.3	25.3	-23	9	-18		
Saquinavir	4	0.5	5.6	11.0	0.5	5.6	11.1	-2	1	-1		
Vinblastine	5	1.0	13.2	13.5 (1.8)	0.9	12.3	14.0	-11	7	-4		
Vincristine	<10	0.9	3.5	4.2	0.9	3.3	3.5	11	6	15		

(i) indicates the presence of Ko143 1 µM.

[a] BCRP substrate and non-substrate ref. source: Merino et al., 2005; Choudhuri et al., 2006.

[b] ER from MDCK-bcrp bidirectional assay was given in parentheses, where ER ≥ 2 is considered as the boundary for substrates.

[c] Pharmacokinetic data following p.o. administration from Bcrp knock out (KO) versus wild type (WT) mice. The *in vivo* ref. source: Jonker et al., 2002, Zaher et al., 2006, Giri et al., 2008, Merino et al., 2005 and 2006, Oostendorp et al., 2009.

[#] False negative substrate

45

Table 4. **MRP2 substrate classification based on Caco-2 permeability in the presence and absence of 10 μM MK571.** P_{app} values were presented as mean with CV% $\leq$15 in triplicate. Drugs were classified based on the criteria in Table 2.

Compound[a]	%FA	P_{app}A-B nm/s	P_{app}B-A nm/s	ER (ATPase[b])	P_{app}A-B nm/s(i)	P_{app}B-A nm/s(i)	ER(i)	TSI$_{PappA-B}$	TSI$_{PappB-A}$	TSI$_{ER}$	AQ
Major substrate											
ActinomycinD	5	0.8	8.0	9.8	2.3	10.1	4.4	178	-25	55	
Amrinone	93	11.7	16.6	1.4	19.4	13.3	0.7	66	22	52	0.4
Daunorubicin	10	1.0	4.0	4.0	2.7	3.2	1.2	165	19	69	0.6
Dipyridamole	66	4.2	22.0	5.3	14.3	20.6	1.4	244	6	73	0.7
Domperidone	93	5.2	15.4	3.0 (3)	7.0	10.3	1.5	35	33	50	0.3
Fluvastatin	98	1.5	15.3	10.3	6.5	6.3	1.0	338	59	91	0.8
Furosemide	61	0.6	13.6	21.4	1.9	5.9	3.1	200	57	86	
HBED	5	0.0	0.1	4.0	0.0	0.1	1.4	99	32	66	0.5

46

Compound[a]	%FA	P_{app}A-B nm/s	P_{app}B-A nm/s	ER (ATPase[b])	P_{app}A-B nm/s(i)	P_{app}B-A nm/s(i)	ER(i)	TSI$_{PappA-B}$	TSI$_{PappB-A}$	TSI$_{ER}$	AQ
Saquinavir	4	0.8	11.7	14.6	1.3	9.2	7.1	62	21	51	
Sulfasalazine	13	0.7	18.6	28.4 (9)	1.8	19.3	10.6	178	-4	63	
Sulindac	90	2.0	14.5	7.4	2.7	7.8	2.9	37	46	60	
Teniposide	0	0.8	12.2	14.9	1.4	9.6	6.9	70	21	54	
Topotecan	30	0.9	12.1	12.9	2.2	11.0	5.0	131	10	61	
Valsartan	40	0.5	2.2	4.8	0.6	1.0	1.6	36	54	66	0.3
Partial substrate											
Etoposide	25	0.6	3.0	4.8	0.9	3.1	3.5	42	-4	27	
Paclitaxel	6	1.1	14.8	14.1	1.7	14.6	8.4	67	1	41	
Ritonavir	66	3.7	15.9	4.3	5.8	13.8	2.4	56	14	45	
Sulfinpyrazone	85	1.7	5.8	3.3	2.3	4.4	2.0	30	23	41	0.2
Non-substrate											
Ciprofloxacin	69	2.0	11.3	5.7	2.1	11.1	5.3	4	2	6	

47

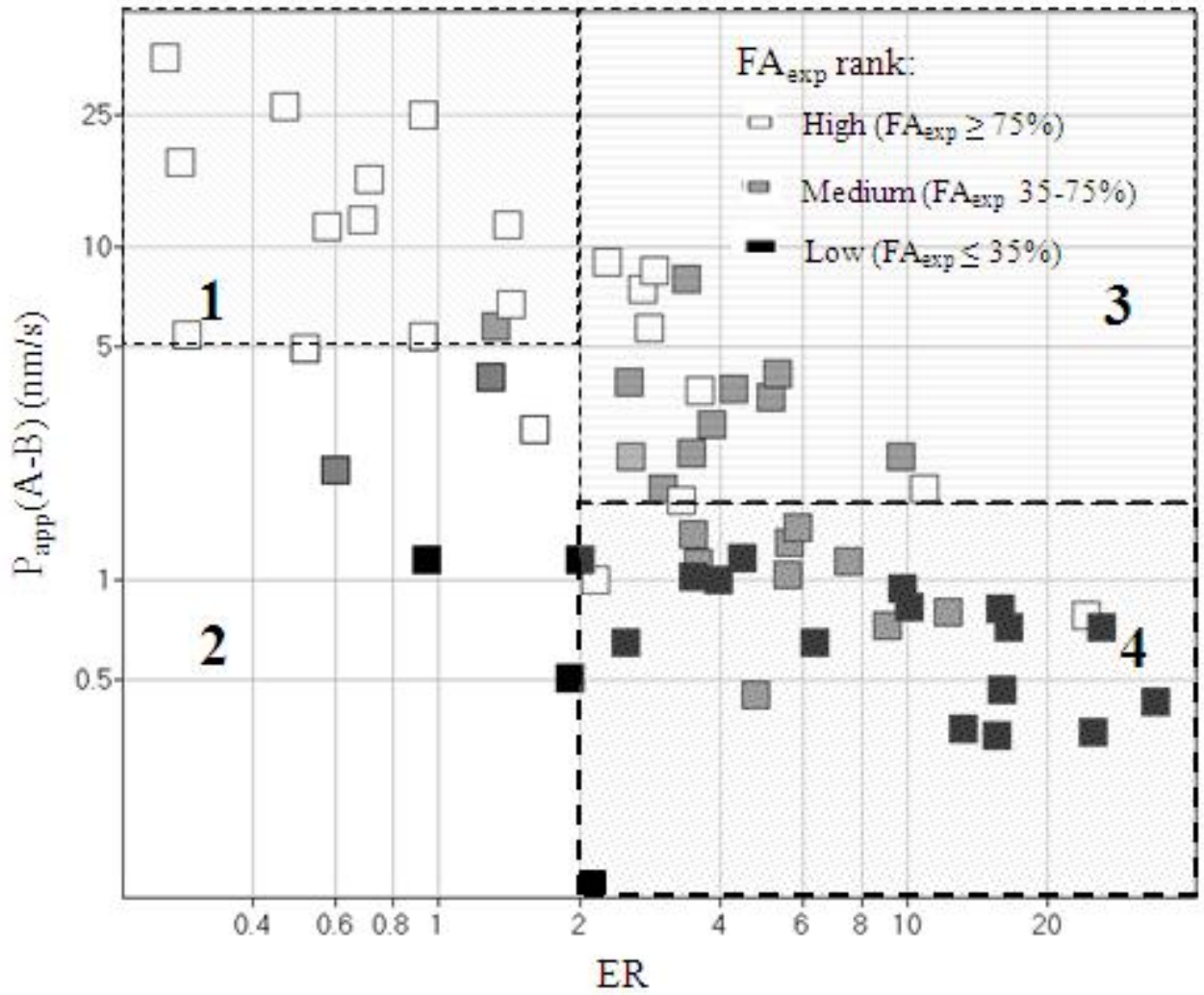| Compound[a]	%FA	P_{app}A-B nm/s	P_{app}B-A nm/s	ER (ATPase)[b]	P_{app}A-B nm/s(i)	P_{app}B-A nm/s(i)	ER(i)	$TSI_{PappA-B}$	$TSI_{PappB-A}$	TSI_{ER}	AQ
Colchicine	44	1.3	5.4	4.3 (-0.4)	1.4	5.6	4.2	8	-5	3	
Erythromycin	35	1.1	8.1	7.1 (1)	1.1	6.8	6.0	0	16	15	
Imatinib	67	3.9	9.5	2.4	3.7	7.5	2.1	-7	21	15	
Methotrexate	20	1.2	1.1	0.9 (-0.2)	1.5	1.2	0.8	30	-11	14	
Metolazone	64	1.8	13.3	7.3	2.2	12.7	5.9	19	4	19	
Nitrofurantoin	100	1.1	11.1	10.4	0.6	9.9	15.8	-41	11	-52	
Norfloxacin	40	1.9	8.1	4.4	2.1	6.7	3.2	15	17	28	
Prazosin	100	6.8	17.2	2.5	8.4	14.0	1.7	24	19	34	

(i) indicates the presence of 10 µM MK571.

[a] MRP2 substrate and non-substrate ref. source: Choudhuri et al., 2006.

[b] MRP2-ATPase assay results with fold activity change over control were given in parentheses, where a compound was classified as an activator if the change was greater than 2-fold.
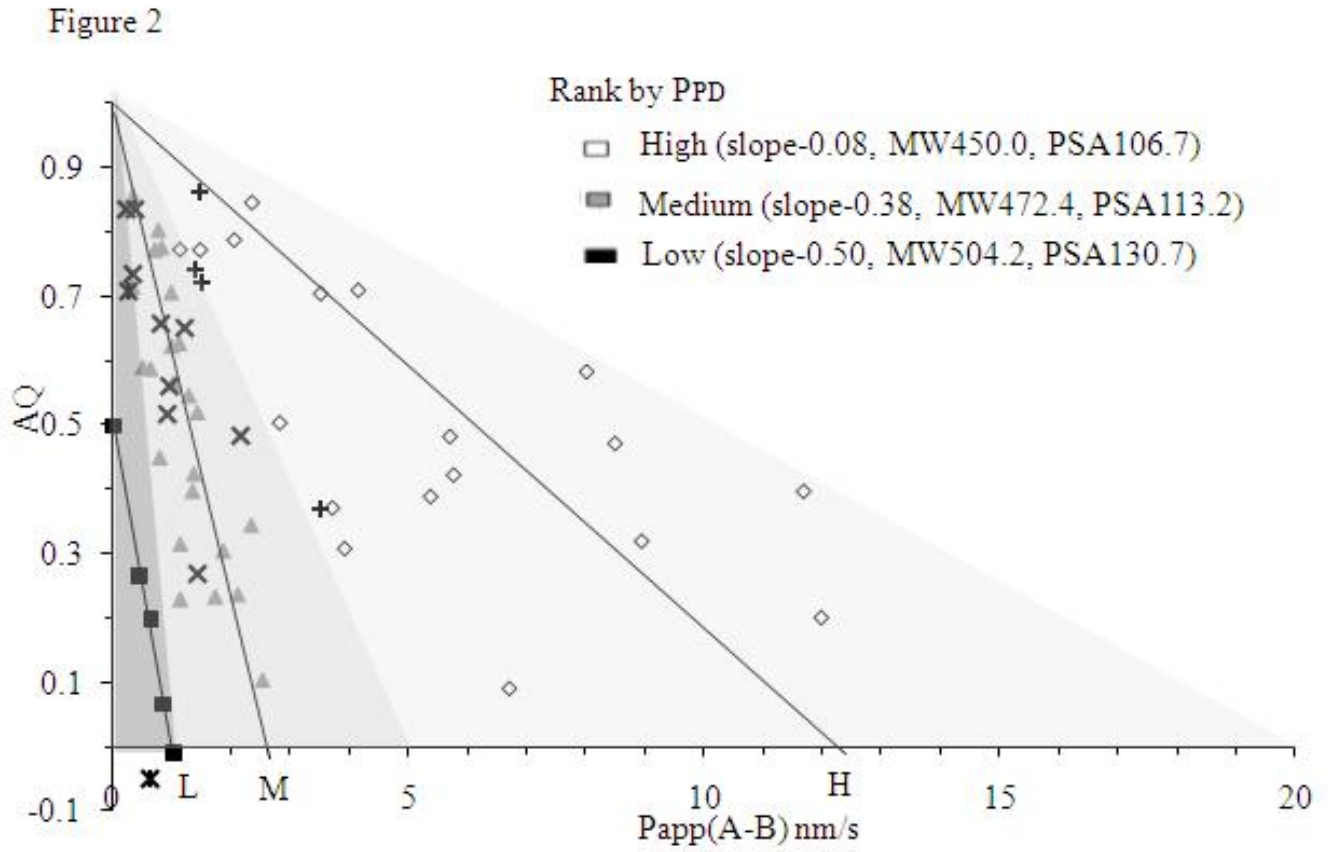
DMD #34629

Figures

Figure 1

DMD #34629

Figure 2

Figure 3